Virtual Reality Training for the Diagnosis of Prostate Cancer

Grigore Burdea, George Patounakis, Viorel Popescu
Human–Machine Interface Laboratory, CAIP Center,
Rutgers–The State University of New Jersey
P.O.Box 909, Piscataway, NJ 08855.
and
Robert E. Weiss M.D.
Department of Urology, R.W. Johnson Medical School,
University of Medicine and Dentistry of New Jersey (UMDNJ),
New Brunswick, NJ 08903.

Abstract

Prostate cancer is the second leading cause of cancer death among men (25% of men with prostate cancer will die of the disease). The most common method of detecting this malignancy is digital rectal examination (DRE). Current DRE training requires medical students to examine a large number of patients before attaining adequate experience. We propose to solve this problem using a virtual reality digital rectal examination simulation. The prototype system consists of a PHANToM haptic interface which provides feedback to the trainee's index finger, a motion restricting board and an SGI workstation, which renders the patient's anatomy in the region of interest. Four types of prostate were modeled using OpenGL and GHOST haptic library– normal, enlarged with no tumor, incipient malignancy (single tumor), and advanced malignancy (tumor cluster). Results of initial human factors studies are encouraging, while pointing out the need for more realistic physical modeling.

1 Introduction

Prostate cancer is the second leading cause of cancer death among men, with 25% of patients dying from the disease [1]. Early detection of prostate cancer is done most commonly by digital rectal examination (DRE), trans-rectal ultrasound and prostatic specific antigen (PSA). DRE in combination with PSA has been shown to be the most cost efficient screening method for prostate cancer [11].

Many medical schools consider DRE a very important diagnostic tool, especially since up to 50% of palpable prostate nodules turn out to be malignant [6]. Finding patients willing to allow medical students to train on them is, however, difficult. DRE maybe uncomfortable for the patient if performed by an inexperienced examiner. Furthermore, the doctor that is training the student has no way of evaluating the student's ability to palpate pathology within the rectum, so mistakes cannot be corrected. Evaluating the improvement of the student's DRE skill is difficult and subjective at best. Therefore, many general physicians are not confident in their ability to perform DRE. This leads to expensive referrals to specialists for prostate evaluation [8].

The solution we propose to this problem is a virtual reality prostate palpation simulation. This training system would provide the same kind of advantages that flight simulators do [8]. There could be a sufficient number of virtual patients and types of malignant prostates to train on at any time. The student would be able to travel inside the patient's body and see the region of interest (rectum, intestine, prostate). This is something that was impossible with the traditional methods of training medical students in DRE. Students training on such a simulator would also feel more comfortable because they are performing the examination on a virtual human being. Studies done on similar tasks show up to 30% decrease in instructor time, up to 30% decrease in student time, and up to 30% increase in student outcome [15]. As more senses are incorporated into a palpation simulation (such as touch and force feedback), the simulation becomes more realistic [19], [14].

Current non-VR palpation simulators used in medical schools, such as Merck's "Procar" simulator, have anatomically accurate rubber models of the prostate which have various beads inserted to simulate malignancies. A plastic cover is used to block the student's view of the phantom during diagnosis, while a rotating plate switches between prostate types [7]. Merril enhanced Merck's mechanical simulator by placing a Polhemus sensor on the trainee's index finger. While force sensation was produced by the mechanical model being palpated, a graphical workstation was used to display a corresponding virtual finger and prostate model [13].

Later, Kaufman at Dalhousie Medical School (Canada) [10] reported the early design of a VR prostate palpation system using a PHANToM haptic interface [12]. The system is presently under development in collaboration with Digital Image FX (Dartmouth, Canada). A commercial version is planned but at the time of this writing no data is available on the completion of the system, or any human factor trials to validate its usefulness.

This paper presents a VR-based training system for prostate palpation developed independently at Rutgers University in collaboration with Robert Wood Johnson Medical School (UMDNJ). Section 2 describes the system components both hardware and software, while Section 3 presents the training approach. Human factor trials on both non-medical students and urology residents from the medical school are analyzed in Section 4. Section 5 concludes this paper.

2 System Components

The components of the VR prostate palpation training system are the haptic interface, the motion restricting board and an SGI workstation. As illustrated in Figure 1, the user interacts with the simulation by placing his finger through a hole in the board and into the PHANToM finger attachment. This force feedback device provides forces to one finger only, which is similar to the use of a single finger in DRE.

The PHANToM version 1 used in our experiments has the smallest work envelope of the three versions which are commercially available. The smaller work envelope was found to be sufficient for this application, due to the constrained nature of the finger motion. While the PHANToM we used did not have fingertip orientation measurement, its position resolution was superior to that of larger versions.

The PHANToM interface box was connected to an SGI High Impact workstation through an ISA card. The high bandwidth of the PHANToM (approximately 1000 Hz) allows it to replicate object surface hardness, texture and different other effects [12]. Its position resolution was also adequate for the range of motions performed during DREs.

The graphics portion of the simulation was developed using OpenGL [16] on a 3-D model purchased

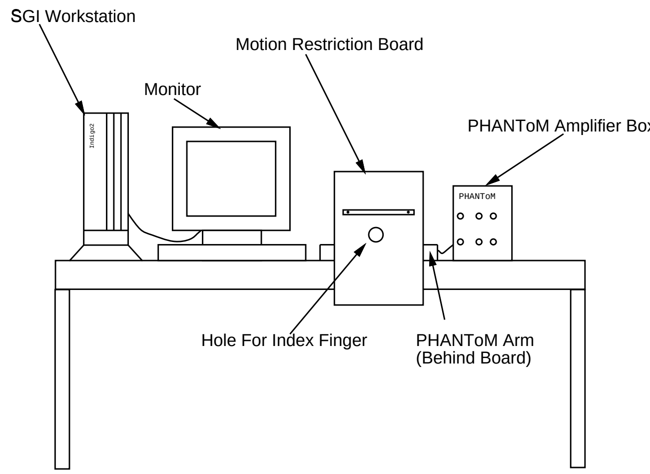

Figure 1. Simulation hardware setup.

from Viewpoint DataLabs [21]. This model consisted of an anatomically accurate adult male, with the urinary tract and intestines. The model was too complex to render in real-time on our mid-range workstation, and had to be simplified. First the body regions which were not of interest were eliminated. These include the lower portion of the legs, the trunk above the waist, the kidneys and the intestine above the rectal region.

In order to show the virtual patient in the same posture as that used in most DREs the waist region was rotated by about 75 degrees, as shown in Figure 2. The buttocks area was interpolated using a "trace" polygonal mesh and then averaging adjacent polygon normals. The final data was stored in a file and loaded at simulation time.

The trainee hand was rendered in low resolution and configured in a fist with the index extended at a fixed angle. Initially the user can see his hand and the virtual patient bent over. Once the user's hand enters the rectal region, and the prostate is in view, only the index finger is shown. The (monoscopic) graphics refresh rate was approximately 18 fps, which was sufficient for our task [17]. No noticeable latencies were present.

Graphics computations are only part of the workstation load. The other important component running on the same SGI is the physical modeling, including contact detection and force feedback computation. The graphics and haptic loops run concurrently but asynchronously, as the haptics loop, which controls the PHANToM, has a much larger bandwidth (about 1000 Hz). The physical modeling task took advantage

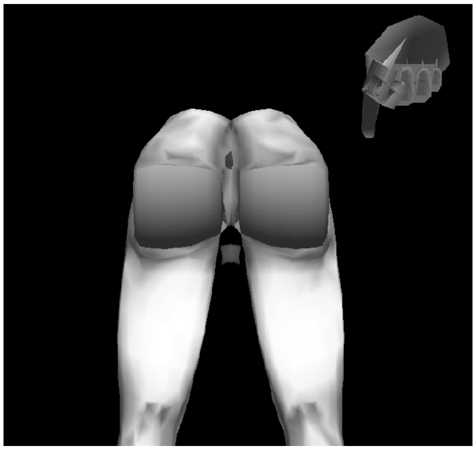

Figure 2. First view in simulation (man bent over).

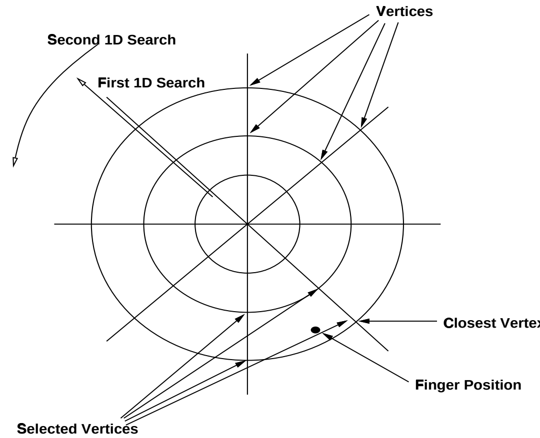

Figure 3. Vertex search optimization.

of the recently introduced GHOST haptic library used to run the PHANToM arm [20]. One limitation in using GHOST was the lack of support for sub-surface forces (as needed to detect hidden harder malignancies). Thus the SGI had to handle both the graphics collision detection and the haptic collision detection load.

In developing the prostate palpation simulation, speed had to be weighted against force feedback realism. These two opposing requirements called for a compromise such that simulation lag was kept small while maintaining sufficient force realism. The constraint imposed by GHOST was that the haptic loop had to be executed at 1000 Hz. Otherwise, GHOST will issue an exit command because the loop is not running quick enough. This constraint limits the complexity of the prostate model that can be used, since the program running on our SGI High Impact could only check approximately 100 vertices for collision detection per haptic loop cycle. Without optimization, this would suggest that the prostate and all the malignancies in it would be limited to an unrealistic level of detail of only 100 vertices.

The optimization used takes advantage of the hemispherical shape of the prostate surface in the area of interest. It assumes that when projected onto a two dimensional surface, the prostate has the shadow of concentric circles. Once this is assumed, the previous two-dimensional search for collision location with the fingertip is now cut down to two one-dimensional searches. The result is a reduction in the computation time by an order of magnitude. As illustrated in Figure 3, the search first finds the closest concentric circle to the fingertip, then searches for the closest vertex on that circle.

The modeling of the prostate and cancers is accomplished by generating the vertices of a hemisphere and then connecting them into four-sided polygons. A median groove is simulated by depressing all the vertices that lie on a single line of longitude of the prostate. After the polygons have been constructed, the normals to the surfaces are calculated. The vertex normals are then calculated by averaging all the surrounding surface normals. This model can be used for both graphics rendering and haptics rendering. The complexity of the model for the prostate is 200 vertices, while each malignancy was constructed with 100 vertices.

The prostate model can be deformed graphically if the virtual fingertip is in contact with it. This is accomplished by using the haptic loop's vertex collision data to displace the vertex the finger came in contact with. The magnitude of deformation is determined by the distance the finger penetrates the surface at the collision location. The surrounding vertices are deformed less and less, as the distance from the point of collision increases. This gives the illusion that the prostate is being graphically compressed by the fingertip.

Once the vertices of the polygon the fingertip is in contact with have been determined, the palpation force magnitude and direction must be computed. The force vector is determined by the following formula:

$$F = k * f(b * d)$$

where k represents the tissue stiffness; d is the penetration distance along the normal defined at the surface point;

$$d = u(< (P_{surfacept} - P_{fingertip}), N_{surfacept} >)$$

u is the unity step function (forces are applied only when the surface is deformed by the fingertip).

The f function models a non-linear deformation. Instead of using Hooke's law, $F = kd$, the simulation uses an *arctan* function for the deformation model. The slope of f can be controlled by the parameter b according to the desired object deformation model. Another useful aspect of the *arctan* function is that it produces bounded forces, avoiding a premature exit due to GHOST safeguards. The normal vector at the point of contact on the surface is determined in a way similar to the Phong shading routine used in graphics [5]. In the simulation, force shading is implemented by calculating a weighted average of the vertex normals closest to the point of contact. The normal vector obtained from this calculation is used to determine the direction of the force the surface exerts on the finger and it is also used as the projection vector for the calculation of the distance the finger penetrated the surface. The magnitude of the force calculated is averaged with the last force magnitude to get an even smoother transition between forces. This is done to eliminate some of the mechanical vibrations or "buzzing" that results from force transitions.

3 Training Simulation

The simulation starts by showing the male patient bent over (the usual DRE position). The trainee must physically insert his finger through the hole in the motion restriction board and into the PHANToM finger attachment. Then the trainee positions the virtual finger on the screen such that it lines up with the rectal area. As the trainee pushes through the anus, the inertia effect starts and the trainee feels resistance. Once the finger has penetrated the rectum, the inertia effect stops and the program switches to an interior view of the patient.

The interior view of the patient consists of a portion of the rectum wire frame so the trainee can see the intestine wall, the prostate, the bladder, and an index finger. If the trainee pushes the virtual finger against the rectum wall, he feels a small resistance to the motion. When the trainee starts palpating the prostate, the prostate model deforms and forces are fed back by the PHANToM. The trainee can feel the median groove which helps orient him hapticly before starting the palpation process.

After the trainee feels confident with the current model being palpated, he can switch to another model with a simple keystroke. The four models that are

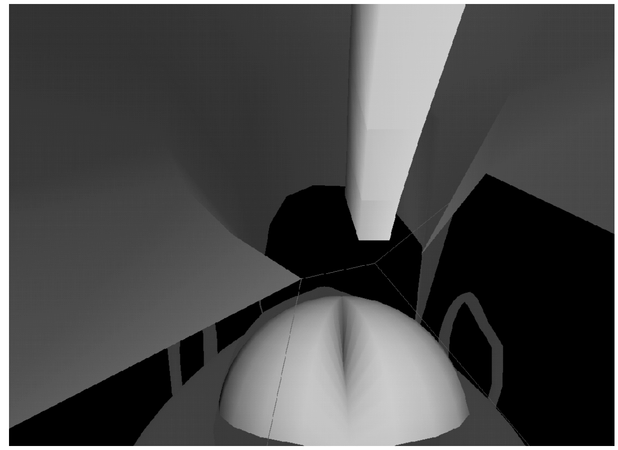

Figure 4. Interior view of an enlarged benign prostate.

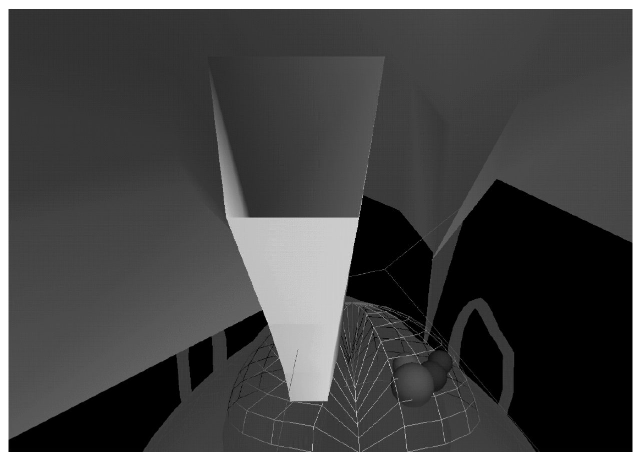

Figure 5. Interior view of a transparent prostate with an advanced malignant cluster.

available for palpation are (small) normal prostate, benign prostatic hypertrophy (enlarged prostate), early cancer nodule (single tumor), and late invasive cancer (a cluster of tumors). The tumor locations are in turn randomized to four different areas (lobes) of the prostate. The trainee has the option of seeing through the prostate surface by turning the model to wire frame rendering.

Once the trainee has palpated each type of prostate, the testing procedure can be started. During testing the screen displays only red or green spheres. The red sphere means "rest" and the green sphere means "palpate." In testing mode, the trainee has to diagnose each case presented to him without seeing the prostate on the screen. All cases are randomized

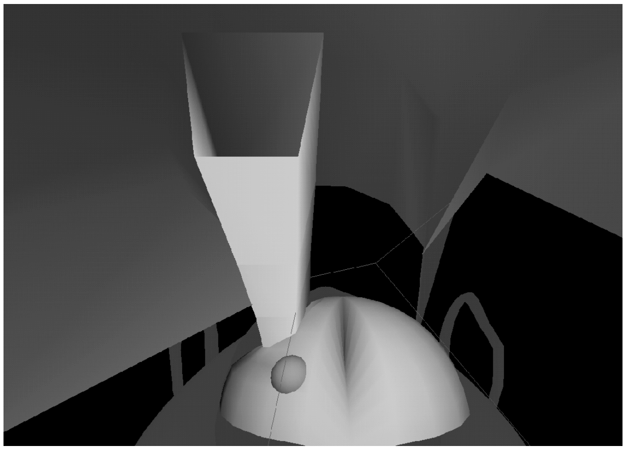

Figure 6. Interior view of a prostate with a single tumor.

by prostate type and by tumor location. The trainee inputs his diagnosis by pressing a key that corresponds to the prostate type. The time it takes for the user to respond is recorded along with the correct diagnosis and the trainee's response.

The test involves twelve randomized prostate cases. Each of the four different prostate cases are presented three times in random order. After the trainee gives his diagnosis, the trainee has a five second break until the next case is presented. The trainee gets a three minute break after every four cases presented. Once the test is done, the results can be viewed by reading a text file that is produced by the program which lists what was recorded during the test.

The trainee's actions can also be recorded to a file which can be played back at a later time. This file records the position of the virtual finger and the case presented at the time. This provides a way to analyze the trainee's palpation technique, and what can be done to correct any errors. It can also be used to record the actions of an expert at prostate palpation to show the trainee exactly how it is done. To playback a recorded file, the simulation simply changes the source of its input from the PHANToM to the data file.

4 Human Factor Studies

Two studies were conducted using the simulation system described above. The first study used non-medical student as subjects, while the subjects in the second study were MD residents at Robert Wood Johnson Medical School (UMDNJ). The subjects in the first study did not use the motion restricting board, while the residents had a harder, but more realistic task which used the board.

The studies were aimed at determining:

1. The trainees' learning curve when using the prostate palpation simulation.
2. Which cases were the most difficult for them to diagnose.
3. The overall accuracy of diagnosis.
4. The time taken to diagnose each case over the three trials.

These goals were selected because they indicate whether the simulation will be useful as a training aid for medical students.

The first study used 22 volunteers, 16 male subjects and six female subjects. Each subject was given an overview of how to palpate the prostate correctly. They were shown how to do this on phantom (rubber) models of the prostate, then they were told to first identify the median groove and evaluate the size of the prostate. The subjects were then told to scan the prostate surface in small increments looking for nodules that signify tumors.

Subsequently each subjects had five minutes of training on the wireframe model of the prostate made visible on the screen. Subjects were reminded of the correct way of palpating a prostate and presented with all four cases at least twice. During training, subjects were allowed to concentrate on the cases they felt were difficult.

Once the five-minute training period ended, the simulation would blank the screen and display a red sphere signifying the initiation of the test. From this point on, subjects were not instructed on palpation technique. Each subject was presented with twelve random cases with a three-minute break between every four cases. They were not given results until after the experiment was finished. The following data was recorded for each subject:

- The length of time in seconds to make a diagnosis.
- The diagnosis the subject chose.
- The correct diagnosis.

For the first study the total percent correct was 46.2%, total percent correct lenient model (only check if cancer was found or not) was 67.0%, the percent correct for the detection of any tumor was 71.43%, and the percent correct for any non-tumor case was 62.1%. The percent correct for each individual case was 48.5% for the small benign case, 43.4% for benign prostatic hypertrophy case, 57.6% for the single tumor, and 34.8% for the tumor cluster case.

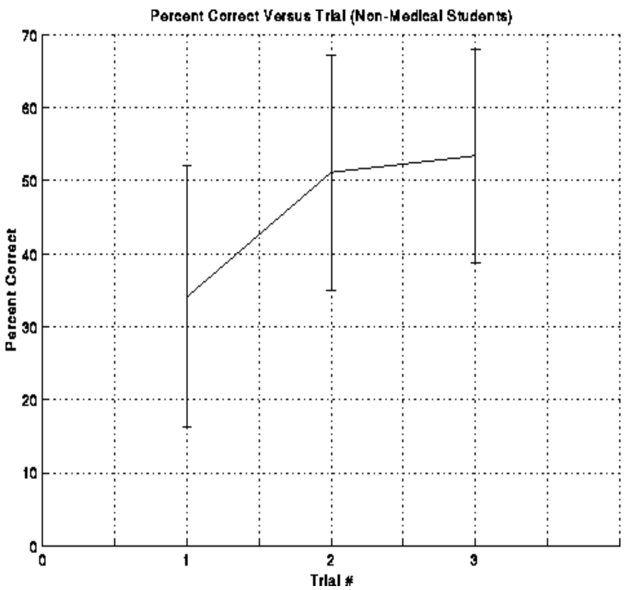

Figure 7. Percent correct diagnosis as a function of trial number.

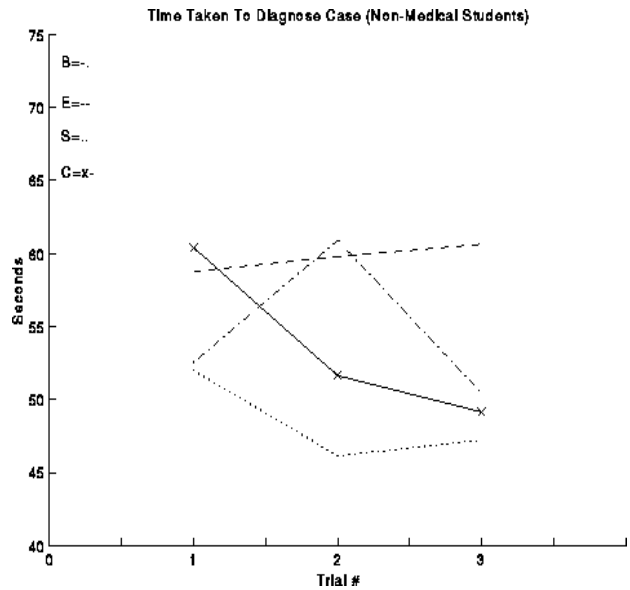

Figure 8. Diagnosis time over the three trials: (-.) small benign prostate, (- -) enlarged prostate, (. .) single tumor prostate, and (- x) cluster or tumors prostate.

This study also showed that learning occurred as subjects went through the three trials. Figure 7 shows the percentage correct overall for each trial became larger as the trials proceeded. It also shows that the standard deviation decreased as the trials proceeded, meaning a more uniform response among the subject population.

Figure 8 shows the time taken to diagnose each individual case over the three trials. The benign case shows a slight decrease in time between the first and third trials, but the average time for the second trial is much larger. This can be explained by assuming that the subjects realized what a small prostate is after the first trial and tried to be more careful during the next trial. Once the mistakes were noted, the time taken to diagnose the case reduced to slightly less than the time for the first trial. The benign prostatic hypertrophy case had a slight increase in time taken for diagnosis. This may be due to more careful searching of the prostate as the subjects progressed in the experiment. Both the cluster tumor case and the single tumor case took less time for diagnosis.

The second study tested four urology resident MDs. The study was conducted using the same protocol as that of the first study, except that the motion restriction board was introduced. The total percent correct diagnosis was now 33.3%, total percent correct lenient model (only check if cancer was found or not) was 56.3%, the percent correct for the detection of any tumor was 63.0%, and the percent correct for any non-tumor case was 54.2%. The percent correct for each individual case was 25.0% for the small benign case, 25.0% for benign prostatic hypertrophy case, 50.0% for the single tumor, and 33.3% for the tumor cluster case.

The lower numbers in the second study may have a number of causes, including tiredness of the subjects (fresh out of OR consultation), and increased difficulty due to the motion restricting board. Another possible explanation is reduced realism of the haptic modeling of the tumors, vs. what the doctors remembered from actual patients. Despite the lower numbers, the data obtained from the percentage correct as a function of trial number still shows learning (see Figure 9). The other graph, diagnosis time as a function of trial number yielded slightly different results (see Figure 10). The small benign prostate was detected in approximately the same amount of time in each trial. The enlarged prostate showed a dramatic decrease in time for detection in this study. The single tumor case took the same time to diagnose in trial one as it did in trial three, but during trial two the time went down slightly. Finally, the cancer cluster case decreased in time taken to diagnose, but had a greater decrease in time for trial two. The two malignant case results can be explained because the subjects were more careful

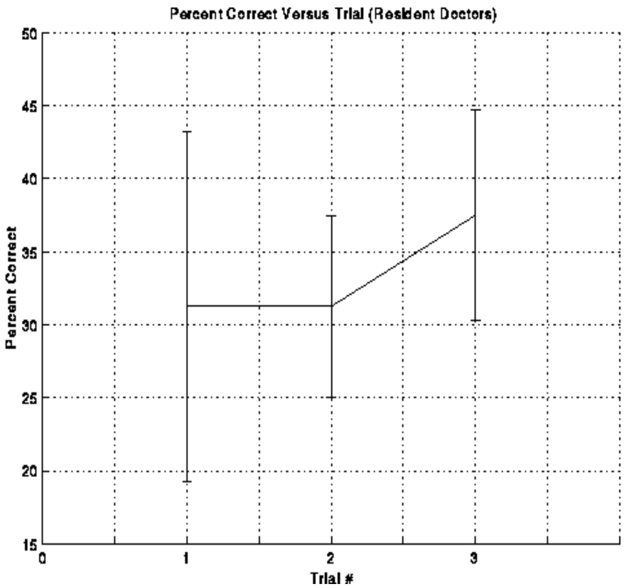

Figure 9. Percent correct diagnosis as a function of trial number.

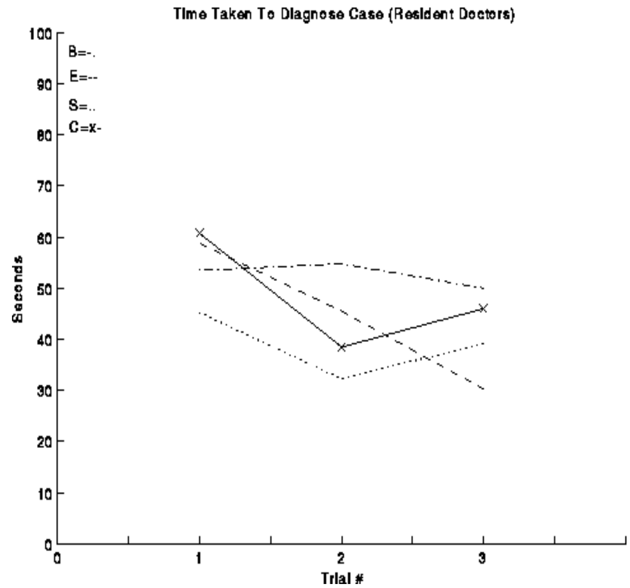

Figure 10. Diagnosis time over the three trials: (-.) small benign prostate, (- -) enlarged prostate, (. .) single tumor prostate, and (- x) cluster or tumors prostate.

in distinguishing between a single tumor and a cluster in the third trial than in the second trial.

Subjects in the second study were also asked subjective questions as to the usefulness and realism of the simulation, as well as perceived problems or difficulties they may have had. Responses were optimistic in terms of eventual usefulness of the system as a teaching aid, provided more realism in the modeling was achieved. One resident had shorter fingers which prevented him from fully palpating the prostate, which we suspect may have happened also in actual DREs.

5 Conclusions

The prostate palpation simulation may provide an important means to improve training doctors in digital rectal examination. Improvements in the haptic modeling of the prostate are necessary for the simulation to become realistic. A way of accomplishing this is to use volumetric haptic rendering instead of surface rendering. Volumetric rendering gives more flexibility for simulating objects that are not realistically modeled by mathematical functions. Although realism is dramatically increased, volumetric rendering increases also computation time and data storage requirements. A volumetric haptic model can be stored in an "octree" spatial partitioning representation [5]. This data structure allows for logarithmic efficiency during the searching of vertices the fingertip is in contact with. Although real forces are recorded in the 3D grid, interpolation is still necessary because forces have to be determined between vertices.

As for the prostate palpation simulation, the forces can be obtained by using the PHANToM to record position and force measurements in a 3D grid. An algorithm can be designed to apply incremental forces to an object and allow it to deform. Once the object has deformed a specified distance, the force currently applied to the object through the PHANToM is recorded. Unfortunately, this type of 3D force and position sampling will not be very accurate with the current hardware. A promising device is being developed by Artann Laboratories (New Brunswick, NJ) working with Robert Wood Johnson Medical Center that will record prostate palpation forces during actual DRE [4]. This device will be very useful to increase the realism of the haptic simulation.

Acknowledgments

Research reported here was supported by grants from the CAIP Center at Rutgers University, and by an equipment loan from SensAble Technologies Co.. We are grateful for the useful suggestions made by Matthew Friedman MD. of Georgetown University, and to the urology residents at R. W. Johnson Medical School who donated their time for this study.

References

[1] Bohring, C. and Squires, T. (1993). Cancer statistics. *CA Cancer J Clin 43*, pp. 7–26

[2] Burdea, G. (1996). *Force and Touch Feedback for Virtual Reality.* New York, John Wiley & Sons, Inc.

[3] Burdea, G. and Coiffet, P. (1994). *Virtual Reality Technology.* New York, John Wiley & Sons, Inc.

[4] Cummings, K., Sarvazyan, A., Pantuck, A., Ward, W., and Weiss, R. (1997). Mechanical Imaging: A Novel Device for Prostate Imaging, *Proceedings of the American Urologic Association*, Vol 157, Abstract 478, pp. 122.

[5] Foley, J., van Dam, A., Feiner, S., and Hughes, J. (1990). *Computer Graphics: Principles and Practice*, Second Edition. Addison-Wesley Publishing Company, Inc., New York.

[6] Gomella, L. and Stephanelli, J. (1993). Malignancies of the Prostate. In *Practical Oncology*, pp. 325.

[7] Health Edco, (1997), "Prostate Training Kit," Waco, TX.

[8] Higgins, G., Merrill, G., Hettinger, L., Kaufmann, C., Champion, H., and Satava, R. (1997). New Simulation Technologies for Surgical Training and Certification: Current Status and Future Projections, *Presence–Teleoperators and Virtual Environments*, Vol. 6 No. 2, April 1997, pp. 160–172.

[9] Irby, D., Lippert, F., and Schand, D. (1991). Psychomotor Skills for the General Professional Education of the Physician, *Teaching and Learning in Medicine 3*, pp. 2–5.

[10] Kaufman, D and Bell, W. (1997). Teaching and Assessing Clinical Skills Using Virtual Reality, *Studies in Health Technology and Informatics: Medicine Meets Virtual Reality*, Vol. 39, pp. 467–472.

[11] Littrup, P., Goodman, A., and Mettlin, C. (1993). The Benefit and Cost of Prostatic Cancer Early Detection, *Cancer Journal for Clinicians*, Vol. 43, pp. 134–149.

[12] Massie, T. and Salisbury, J. (1994). The PHANToM Haptic Interface: A Device For Probing Virtual Objects, *Proceedings of the ASME Winter Annual Meeting Symposium on Haptic Interfaces for Virtual Environment and Teleoperator Systems*, DSC-Vol. 55–1, New York, pp. 295–300.

[13] Merril, J. (1993). Demonstration at the American Urologic Association Meeting.

[14] Merril, G., Raju, R., and Merril, J. (1995). Changing the Focus of Surgical Training, *VR World*, March/April 1995, pp. 56–61.

[15] McGovern, K. and Johnston, R. (1996). The Role of Computer-Based Simulation for Training Surgeons, *Studies in Health Technology and Informatics: Medicine Meets Virtual Reality: Health Care in the Information Age*, Vol. 29, pp. 342–345.

[16] *OpenGL Programming Guide: The Official Guide to Learning OpenGL, Release 1*, Addison-Wesley Publishing Company.

[17] Richard, P., Birebent, G., Coiffet, P., Burdea G., Gomez, D., and Langrana N. (1996). Effect of Frame Rate and Force Feedback on Virtual Object Manipulation. *Presence*, Vol. 5 No. 1, Winter 1996, pp. 95–108.

[18] Satava, R. (1995). Medicine 2001: The King Is Dead, *Studies in Health Technology and Informatics: Interactive Technology and the New Paradigm for Healthcase*, Vol. 18, pp. 334–339.

[19] Satava, R. and Jones, S. (1997). Virtual Environments for Medical Training and Education. *Presence*, Vol. 6 No. 2, pp. 139–146.

[20] SensAble Technologies (1997). Company brochure, Cambridge MA.

[21] Viewpoint DataLabs International (1994). Orem, Utah. *Viewpoint Catalog*, Third Edition.